Indian J. Phys. **72B** (6), 571-607 (1998)

REVIEW

IJP B
an international journal

Tropospheric VHF propagation studies over Indian east coast

Swati Choudhury

Machine Intelligence Unit, Indian Statistical Institute, 203, Barrackpore Trunk Road, Calcutta 700 035, India

D Dutta Majumder*

Electronics and Communication Science Unit, Indian Statistical Institute, 203, Barrackpore Trunk Road, Calcutta 700 035, India

and

Amita Pal

Applied Statistics Unit, Indian Statistical Institute, 203, Barrackpore Trunk Road, Calcutta 700 035, India

Received 4 September 1998, accepted 23 September 1998

Abstract : We have recorded the signal value of 188 MHz (VHF) radiowave propagating over a 70 km long radiocommunication link situated between Satkhira TV station (Bangladesh) and Electronics and Communication Sciences Unit of Indian Statistical Institute Calcutta (India) By using some standard statistical method, we have fitted some appropriate distribution to the average value of the VHF signal level We have proposed fitting beta-distribution with appropriate parameters for the months/seasons in which the observed distribution is unimodal On the other hand, for the periods in which the distribution is multimodal, a mixture of normal distribution can be used to model the data In addition to this, we have estimated the average fade-rate and fade-depth of VHF signal for different months and seasons over our experimental site. The discrepancies in fading behavior has been explained on the basis of radioclimatology of the corresponding radioenvironment These results can be very useful for radio engineers and scientists, frequency planners in setting up some additional radio communication links over this region and can also be used to modify the existing radio communication links to get more reliable performance throughout the year

Keywords · Radiowave and microwave propagation, Indian east coast, VHF signal distribution

PACS No. 84 40 -x

PLAN OF THE ARTICLE

1. **Introduction**

* Communicating author . e-mail : ddm @ isical.ac in

1. Introduction

Propagation of electromagnetic waves in different frequency bands has remained a subject of great interest for their wide application in the area of Navigation, Civil-aviation, Communication, Atmospheric sciences and various other related fields [1-4]. A survey of relevant literature reveals that research on radiowave propagation and corresponding radioclimatology has been conducted mainly over the northern region of India and to some extent over the southern region [5-9]. It has been observed that the eastern region of India experiences significant diurnal, monthly and seasonal changes in weather parameters which in turn, affects the radioclimatological behavior of the tropospheric region to a much greater extent. This ultimately influences the propagation characteristics of radiowaves (mainly lying in the upper VHF band and above) in different ways [10-15]. From the above fact we realized the need of conducting experimental research on radiowave propagation and radioclimatology over the eastern coastal region of India.

To set up a reliable radiocommunication link, the radio engineers are required to consult the radiowave propagation model (to have an idea of the average signal situation during different months and seasons over that region) of that region if there exist any. To develop such model one need to have a massive collection of data which can only be achieved through planned experimental studies. Keeping this in mind, we have installed our experimental set up accordingly and the detail description of which is given in the next section of this paper.

Using our experimental set up, we have recorded the VHF signal level for different months and seasons over this region. During the course of data collection we realized that one has to deal with a large amount of data to study the behavior and characteristics of radio signal, propagation over a radiocommunication link situated over a particular region. This large amount of data is useless, unless it is analysed properly to extract the necessary and useful information At the same time, in future if someone wants to set up some additional radiocommunication link over that region it is obvious that he would like to consult previously recorded data, if there exist any, so that he can think and introduce some possible modifications in his newly built links for radiocommunication. In such a situation, it becomes extremely difficult on his part to search through a huge bulk of data to investigate the average signal situation and propagation characteristics of a radiowave, during different months and seasons over a particular region.

To overcome this problem, after extracting the VHF signal value from chart paper we have estimated the percentage occurrences of different VHF signal level for different months and seasons and have also fitted some appropriate statistical distributions. In addition to this we have analysed the VHF signal to visualise its fading characteristics during the different months and seasons over this region. The results obtained have been summarized in the final section.

2. The experimental set up to record the VHF TV signal (188 MHz) and collection of data

A 188 MHz TV signal is transmitted regularly from Satkhira TV station, Bangladesh, from 1630 hours to 2230 hours. VHF signal value has been recorded regularly at the Electronics and Communication Science Unit of the Indian Statistical Institute, Calcutta. Figure 1 shows the simple block diagram of the experimental set up used to record the VHF signal level. A highly

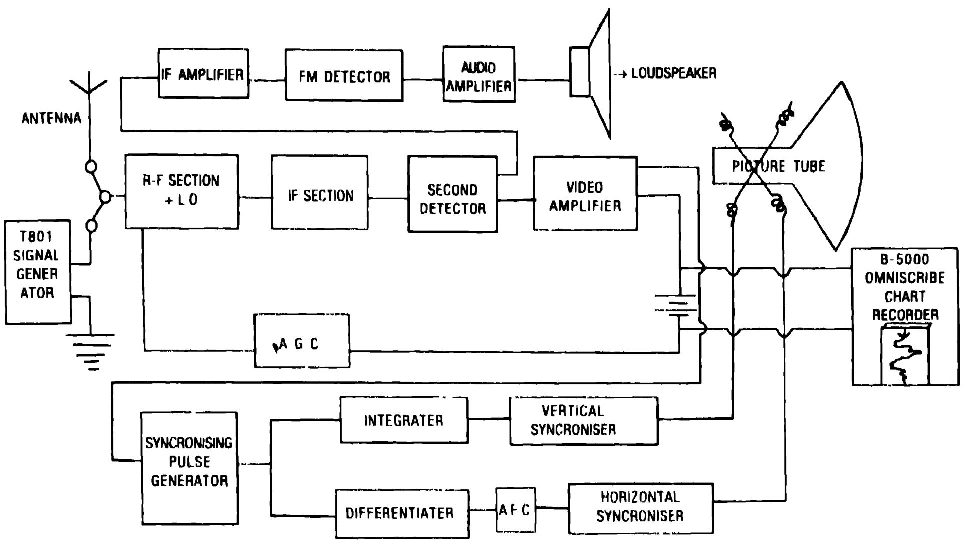

Figure 1 Simple block diagram of the experimental set up used to record the 188 MHz VHF signal level

directional yagi antenna situated over the 30 meter high building of the Institute has been used to receive the signal. Effective radiated power of the 150 meter tall transmitting antenna is 2 kilowatts. The distance between transmitting and receiving antenna is 70 km approximately. Figure 2 describes the geographical location of transmitting and receiving stations. The distance between transmitting and receiving antenna consist of plane land, vegetable and paddy fields. It is free from any hilly terrain and mountain ranges.

The receiver used here is a simple monochrome TV receiver. A delayed A.G.C. circuit connected between RF, IF and video amplifier circuit of the receiver, controls the gain of the receiver in such a way that a signal of substantially constant value persists at the output stage of the receiver. It enables tuning to the station of varying signal strength without any appreciable change in the size of the output signal. It also wipes out input signal variations, so that a moderately steady signal can be obtained at the output stage. Variation in A.G.C. bias voltage which finally changes the receiver gain, is directly proportional to signal fading and is recorded on chart paper with the help of 5000-B type omniscribe strip chart recorder. At the recorder input, a buck voltage (which can be varied within a range) has been applied to compare the A.G.C. variation. Deflection of the pen or the marker on the chart paper is directly proportional to the voltage difference between A.G.C. input stage and the buck voltage and finally describes the fading characteristics of the VHF signal received by the system.

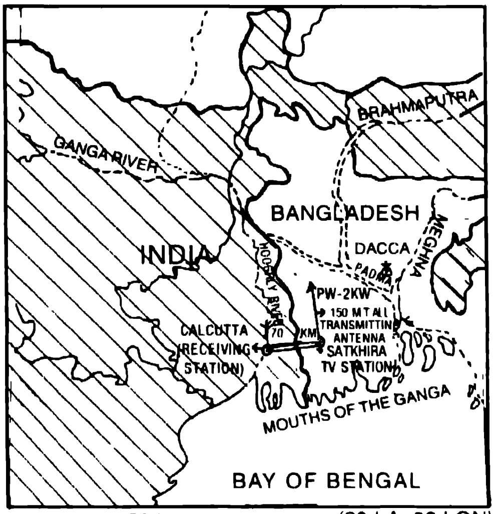

Figure 2 Geographical location of the transmitting and receiving station

2.1. Seasonal and monthly VHF signal level variation

Figures 3 and 4 present the cumulative distribution of average VHF signal level for Satkhira-Calcutta TV link for the years 1986 and 1987 respectively. These figures show that the pre-monsoon season exhibits the highest signal values followed by winter season. This is followed by post-monsoon season with monsoon season exhibiting the lowest value. Figure 3 shows that VHF signal exceeds about 38 db (with respect to 1 microvolt) for 94% of the time in the pre-monsoon season whereas it exceeds about 31 db for the same percent of time during the monsoon season. Similarly Figure 4 shows that VHF signal exceeds about 38db for 90% of time in pre-monsoon season whereas, it exceeds about 32 db for the same percent of time during monsoon season.

Figures 5-16 represent the distribution of percentage occurrence of the average VHF signal for all the twelve months (from January to December respectively) and the figures 17-20 present the same for the four different season (pre-monsoon, monsoon, post-monsoon and winter). In these figures a part represents the year 1986 whereas the b part presents the year 1987. We have discussed the discrepancy in seasonal behavior of percentage occurrence of average VHF signal through Figures 3 and 4. In these figures continuous curves (referred to as experimental curves in the figures) are obtained by analysis of VHF data collected on a regular basis at our site of experiment whereas dotted curves (which referred to as fitted curves) are obtained by fitting an statistical distribution on VHF data by using an appropriate statistical method.

As far as the monthly behavior of average VHF signal is concerned, we can observe that during the month of October about 71 % of time the average VHF signal level has persisted

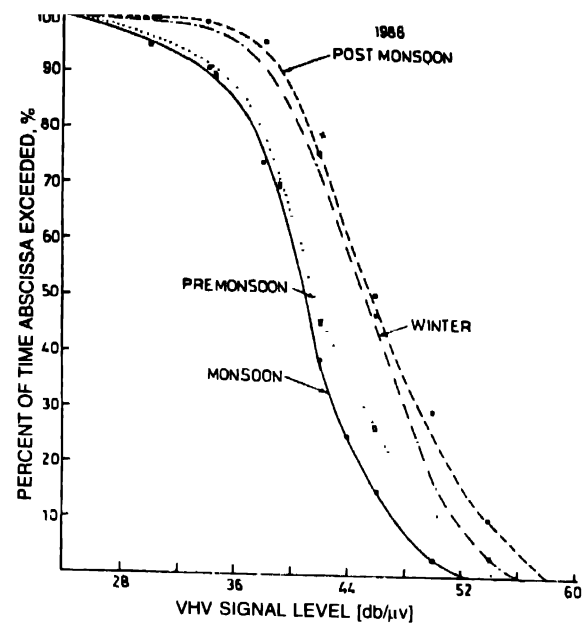

Figure 3 Cumulative distribution of the average VHF signal level for Satkhira-Calcutta TV link, 1986

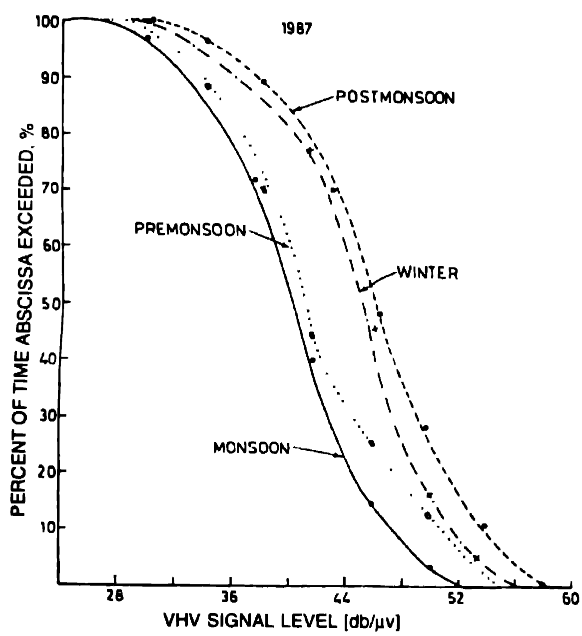

Figure 4. Cumulative distribution of the average VHF signal level for Satkhira-Calcutta TV link, 1987

above 45 db whereas during the month of June and November the average VHF signal level has persisted above 45 db only for 27% and 15% of time respectively.

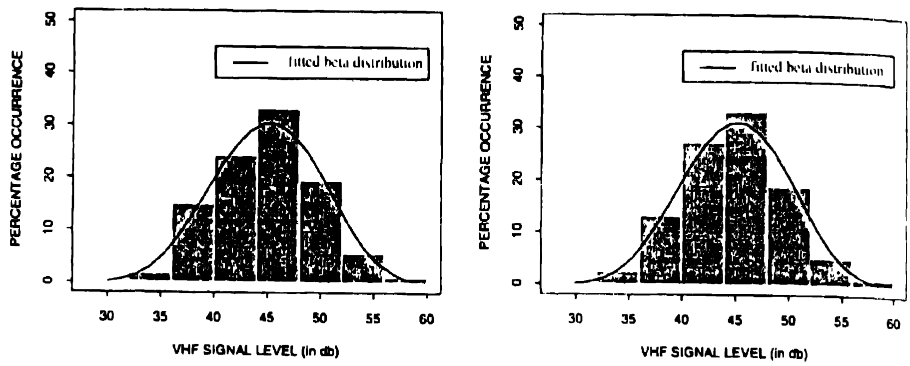

(a) For the year 1986 (b) For the year 1987

Figure 5 Distribution of the average VHF signal level during the month of January, 1986 and 1987

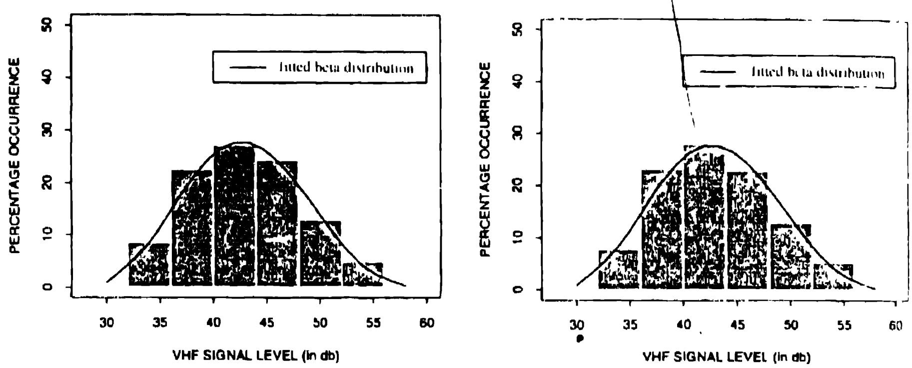

(a) For the year 1986 (b) For the year 1987

Figure 6 Distribution of the average VHF signal level during the month of February, 1986 and 1987

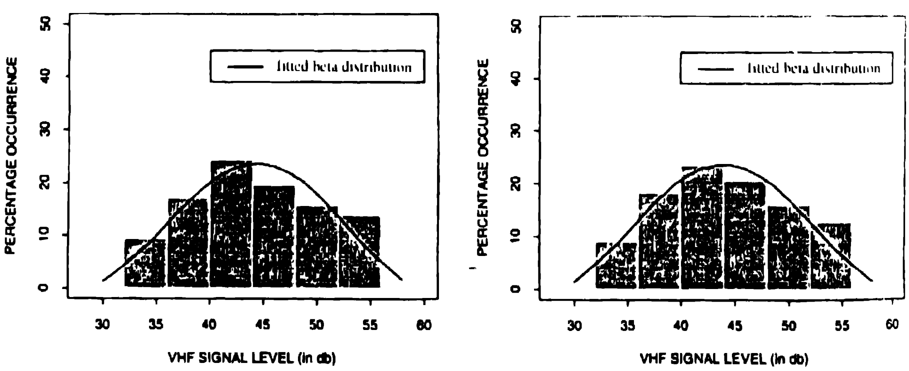

(a) For the year 1986 (b) For the year 1987

Figure 7 Distribution of the average VHF signal level during the month of March, 1986 and 1987

2.2. Fitting a statistical distribution to the average VHF data :

On the basis of the discussion and the presentation of the figures depicting the distribution of the average signal strength in different months in the preceding section, the following

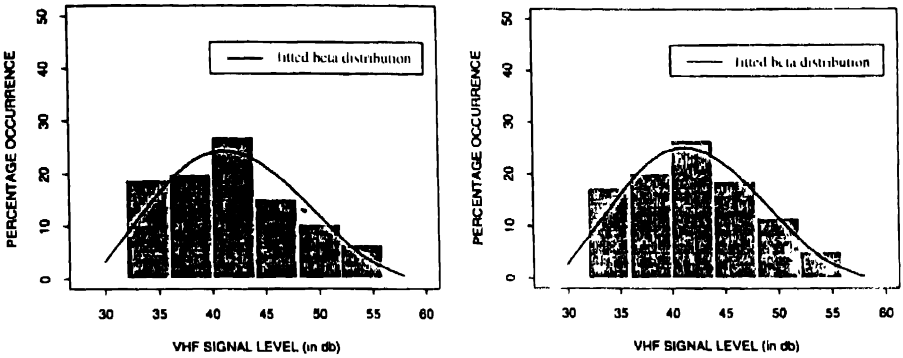

(a) For the year 1986 (b) For the year 1987

Figure 8 Distribution of the average VHF signal level during the month of April, 1986 and 1987

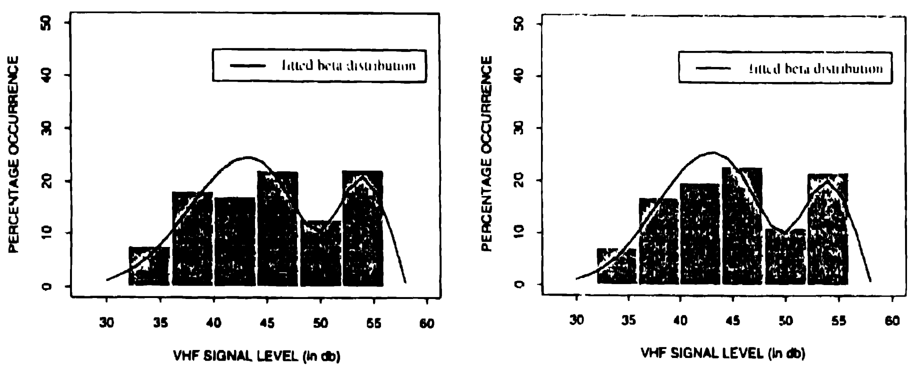

(a) For the year 1986 (b) For the year 1987

Figure 9. Distribution of the average VHF signal level during the month of May, 1986 and 1987

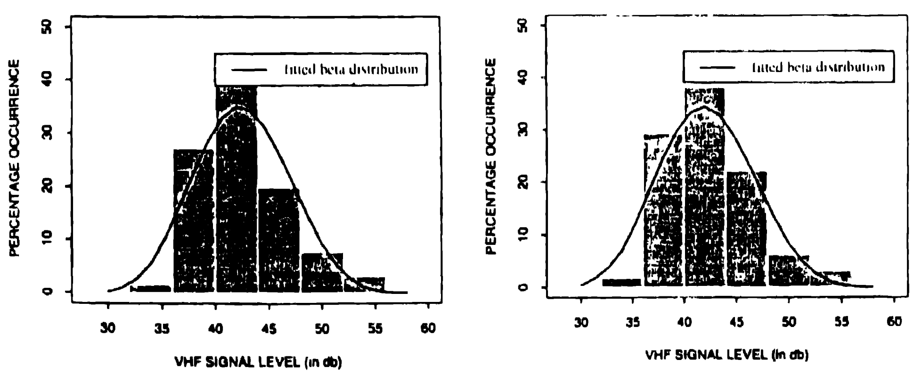

(a) For the year 1986 (b) For the year 1987

Figure 10 Distribution of the average VHF signal level during the month of June, 1986 and 1987 observations could be readily made regarding the average VHF signal data (monthly and seasonal) over the years 1986 and 1987 :

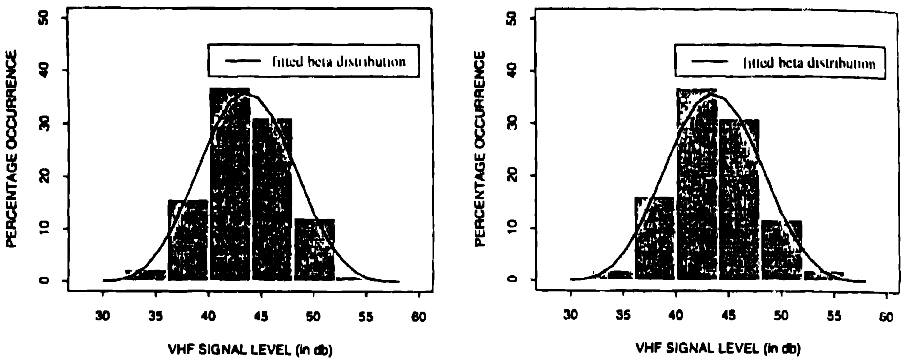

(a) For the year 1986 (b) For the year 1987

Figure 11 Distribution of the average VHF signal level during the month of July, 1986 and 1987.

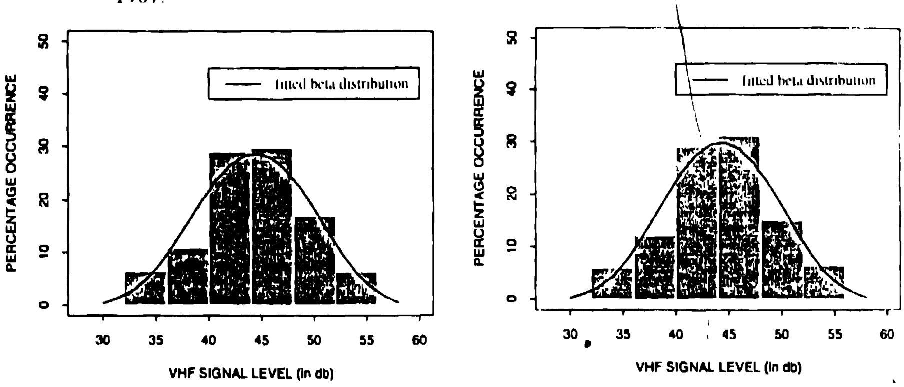

(a) For the year 1986 (b) For the year 1987

Figure12 Distribution of the average VHF signal level during the month of August, 1986 and 1987

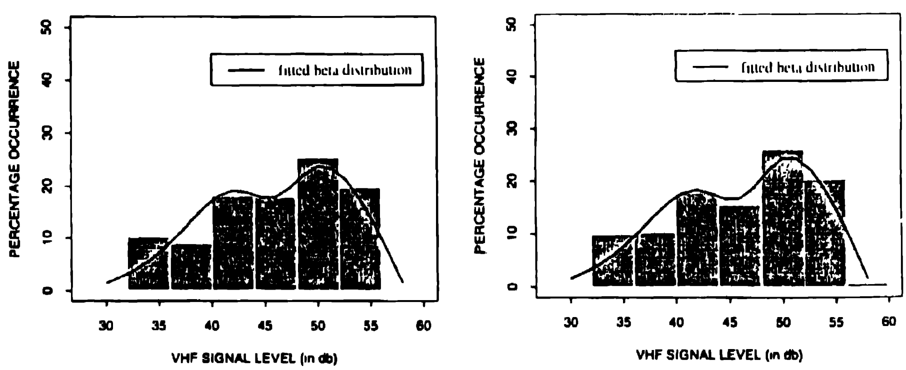

(a) For the year 1986 (b) For the year 1987

Figure 13. Distribution of the average VHF signal level during the month of September, 1986 and 1987

The data was seen to exhibit more or less similar patterns of behavior in corresponding months as well as seasons, over the two years under study. Moreover, the distributions of %

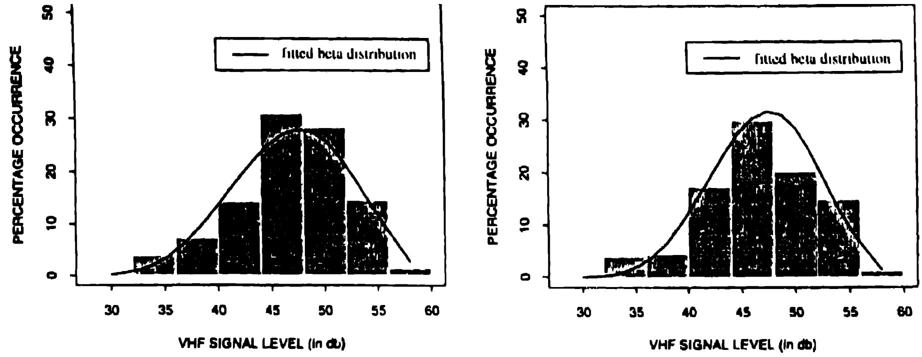

(a) For the year 1986 (b) For the year 1987

Figure 14 Distribution of the average VHF signal level during the month of October, 1986 and 1987

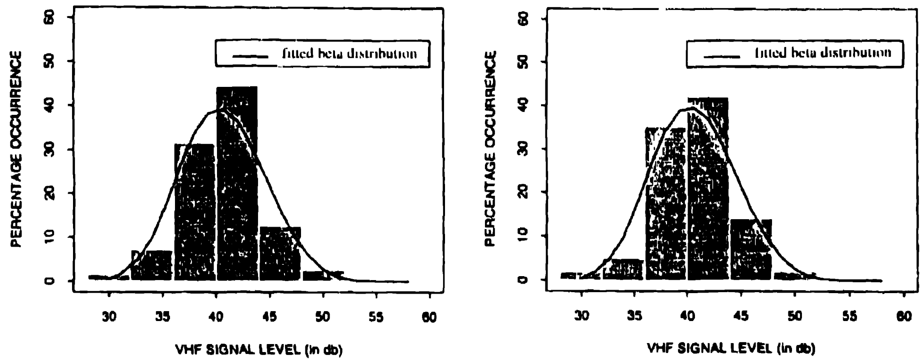

(a) For the year 1986 (b) For the year 1987

Figure 15 Distribution of the average VHF signal level during the month of November, 1986 and 1987

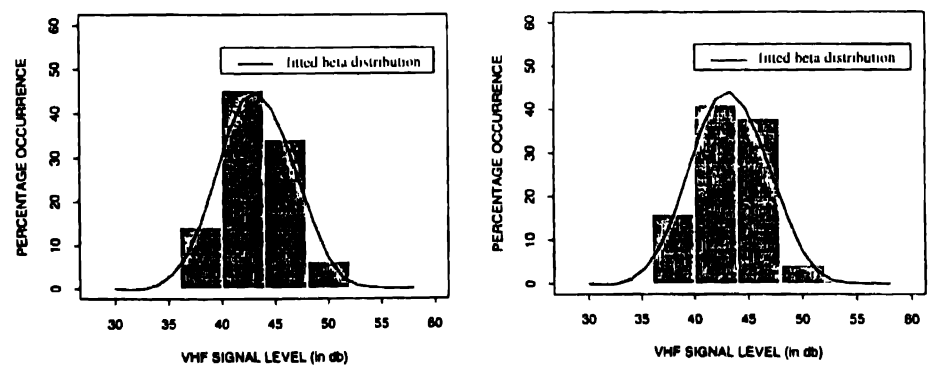

(a) For the year 1986 (b) For the year 1987

Figure 16 Distribution of the average VHF signal level during the month of December, 1986 and 1987 occurrence exhibit differing characteristics over different months and seasons. For instance, in the monthly data, it was seen that for some months, the distribution was unimodal and negatively

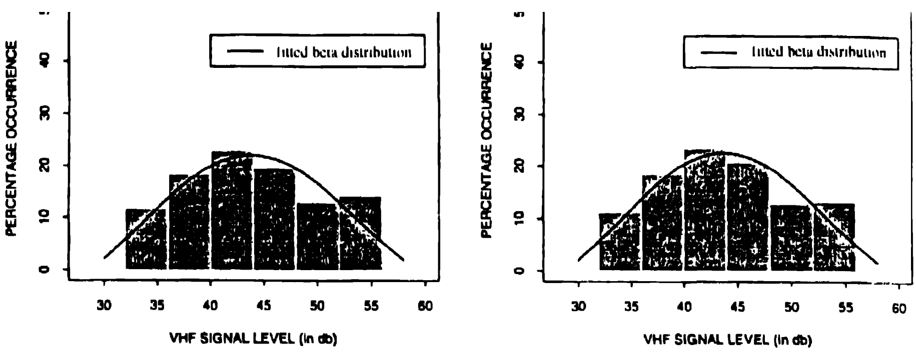

(a) For the year 1986 (b) For the year 1987

Figure 17 Distribution of the average VHF signal level during the pre-monsoon season, 1986 and 1987

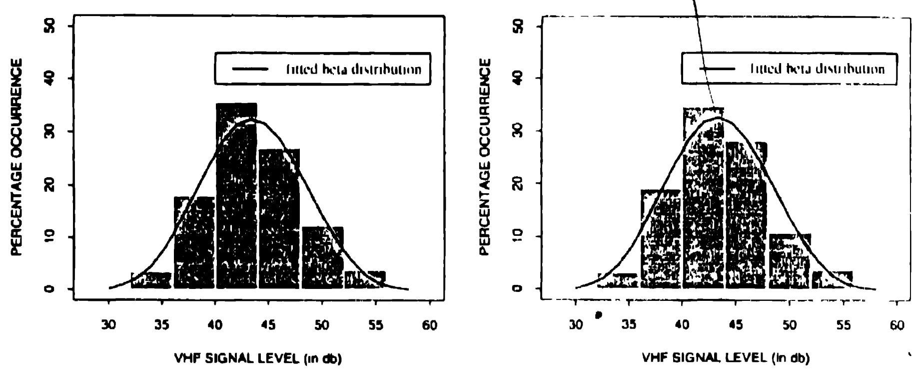

(a) For the year 1986 (b) For the year 1987

Figure18 Distribution of the average VHF signal level during the monsoon season, 1986 and 1987

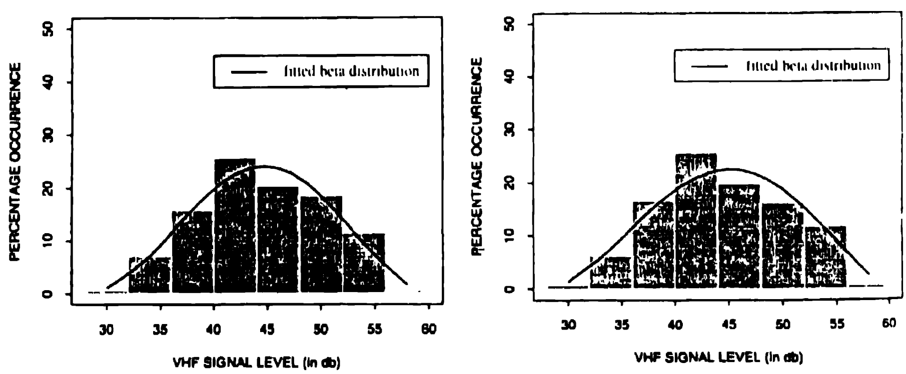

(a) For the year 1986 (b) For the year 1987

Figure 19. Distribution of the average VHF signal level during the post-monsoon season, 1986 and 1987

skewed, whereas in other months, *e.g.*, in January 1986 and 1987 it is unimodal and in September 1986 and 1987, it is bimodal in nature.

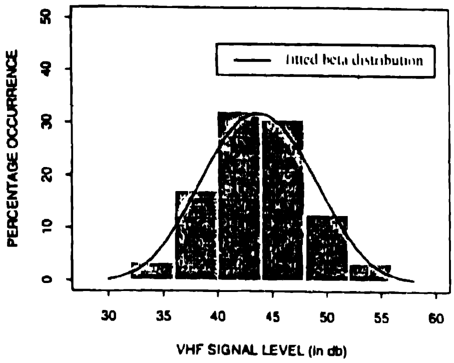

(a) For the year 1986

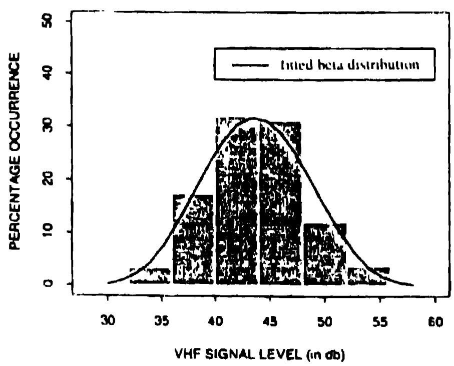

(b) For the year 1987

Figure 20 Distribution of the average VHF signal level during the Winter season, 1986 and 1987

As far as the unimodal distributions were concerned, after a scrutiny of the different types of distribution observed, it was felt that perhaps the two-parameter *beta family of distributions* over the interval [0,1] is most appropriate for describing the varying nature of the observed family of VHF signal distributions, after appropriate transformation of the variable, so as to make its range of variation in the closed interval [0,1].

This is because, for different choices of the two parameter p and q, the beta distribution, described by the probability density function given in the following section, gives rise to a variety of curves, which include all instances of the observed VHF distribution curves [16]. Hence, the beta distribution was chosen to model the VHF data, both monthly and seasonal, in cases where the data was seen to be unimodal.

Similarly, for the multimodal distributions, we assumed the probability model to be a mixture of appropriate normal distributions, namely,

$$P_i(\omega) = \sum^{g} \pi_i f(\omega, \mu_i, \sigma_i) = \sum^{g} f_i(\omega) \tag{1}$$

where,

g = the number of modes,

π_i = the mixing parameter,

$$0 < \pi_i < 1, \sum_{i=1}^{g} \pi_i = 1$$

and

$$f(\omega, \mu_i, \sigma_i)$$

is the Normal distribution with parameters μ_i and σ_i, its functional form being

$$f_i(\omega) = f(\omega\,;\mu_i,\sigma_i) = \frac{1}{\sigma_i\sqrt{2\pi}}\, e^{-\frac{1}{2\sigma_i^2}(\omega-\mu_i)^2}, -\infty < \omega < \infty\,. \tag{2}$$

2.3. The beta distribution :

The family of beta distributions is composed of all distributions with probability density functions of form

$$P_1(y\,;p,q) = P_1(y) = \frac{1}{B(p,q)}\,\frac{(y-a)^{p-1}\,(b-y)^{q-1}}{(b-a)^{p+q-1}}$$

$$(a \le y \le b)$$

with $p > 0$, $q > 0$, $B(p, q)$ being the beta function with parameters p and q, defined by

$$B(p,q) = \int_0^1 x^{p-1}(1-x)^{q-1}\,dx\,. \tag{3}$$

If we make the transformation

$$X = (y-a)/(b-a),$$

we obtain the probability density function

$$P_1(x\,;p,q) = \frac{1}{B(p,q)}\,x^{p-1}\,(1-x)^{q-1}, \tag{4}$$

$$(0 \le x \le 1)$$

wherever there is no scope for confusion, we shall denote $P_1(x;p,q)$ by $P_1(x)$ only for the sake of brevity. This is the standard form of the beta distribution with parameter p and q.

To estimate the value of the parameters p and q, we have used the method of moments which is described briefly below.

2.4. Method of moments for the estimation of parameters .

Let $X_1, X_2, \ldots, X_n$ be a random sample from a population characterised by the probability density function (p.d.f.) f_θ, where $\theta = (\theta_1, \theta_2, \ldots, \theta_k)$. Then the *r-th* order sample central moment m_r is defined as

$$m_r = \frac{1}{n}\sum (X_i - \bar{X})^n$$

while the *r-th* order population central moment μ_r is defined as

$$\mu_r = E(X-\mu_1')^r$$

where,

$$\mu_1' = E(X),\;\; r = 0, 1, 2, \ldots$$

Let the first k population moments exist as explicit functions of the parameters :

$$\mu_1' = \mu_1' (\theta_1, \ldots, \theta_k),$$

$$\mu_r = \mu_r (\theta_1, \ldots, \theta_k),$$

for

$$r = 2, 3, \ldots, k.$$

In the method of moments, we equate k sample moments to the corresponding population moments. Generally, the first raw moments about zero and the second to the k^{th} central moment are equated.

Thus the equations are

$$\mu_1' \leq \bar{X}$$

and

$$\mu_r = m_r$$

for $r = 2, 3, \ldots, k$.

For the standard beta distribution, the r-th order moment about zero can be expressed as

$$\mu_r' = \frac{B(p+r, q)}{B(p, q)}$$

$$= \frac{\Gamma(p+r)\,\Gamma(p+q)}{\Gamma p \Gamma(p+q+r)} \tag{5}$$

$$= \frac{p^{[r]}}{(p+q)^{[r]}}$$

where r is any integer ≥ 0 as before and $\Gamma(x)$ stands for the gamma function with parameter x. The equations for obtaining the estimates of the parameters p and q by the method of moments, are

$$\bar{x} = \frac{p}{p+q} \tag{6}$$

and

$$s^2 = \frac{pq}{(p+q)^2 (p+q+1)}, \tag{7}$$

where

$\bar{X}$ = mean value of the observations,

s^2 = the variance of the observations.

Solving eqs. 6 and 7 for p and q, gives the method of moments estimates of p and q as

$$\hat{p} = k\,\hat{q} \tag{8}$$

$$\hat{q} = \frac{1}{(k+1)}\left[\frac{k}{S^2(k+1)^2} - 1\right] \tag{9}$$

where

$$k = \frac{\overline{X}}{1-\overline{X}}. \tag{10}$$

The estimated values of parameters for the seasons and months for which unimodal data were obtained are given in Tables 2–5.

Table 1. Parameters μ, σ^2 and α of the components of the 2-component normal mixture fitted to the VHF signal level distributions for May and September 1986, 1987

Months	1st component			2nd component			χ^2
	μ_1	σ_1^2	α_1	μ_2	σ_2^2	α_2	
May, 1986	42.98	26.68	0.810	54.00	1.00	0.190	8.827
September, 1986	43.04	31.21	0.695	51.99	4.47	0.305	8.660
May, 1987	42.92	24.61	0.813	54.00	1.00	0.187	6.761
September, 1987	42.57	30.46	0.651	51.95	4.84	0.349	5.983

After estimation the parameters p and q we have used eq. (4) to calculate the beta distribution probabilities P_i for 7 class intervals into which the data has been grouped. This is done by computing for mid points $x_1, x_2, \ldots, x_7$ of the classes the values of the function $F(X) = \int_0^1 P(t)\,dt$ of the beta distribution where $P(t)$ is the probability density function and is given by 4. Thereafter the probabilities P_i, $i = 1, 2 \ldots, 7$ is obtained by equation

$$P_i = F(x_i) - F(x_{i-1}),$$

where $F(x_0)$ is taken to be zero. The fitted beta distributions have been superimposed on the histogram of the data in Figures 5-20 to facilitate the comparison with actual data.

Table 2. Value of the parameters p and q of beta-distribution and the chi-square value for the year, 1986

Seasons	p	q	χ^2
Premonsoon	2.69	2.74	8.64
Monsoon	5.63		
		5.97	2.14
Post monsoon	3.31	3.11	2.29
~~Winter~~	~~5.56~~	~~5.72~~	~~1.37~~

There exist various tests (chi-square Test, Kolmogorov test, the sign test etc.) to confirm whether the observed frequency distribution fits a specified distribution. We have used the chi-square test of goodness of fit to confirm that the average VHF signal level follows a beta distribution.

Table 3. Value of the parameters p and q of beta-distribution and the chi-square value for the year, 1987.

Seasons	p	q	χ^2
Premonsoon	2.81	2 87	7 28
Monsoon	5.67	6 09	1.88
Post monsoon	2.95	2 68	2 52
Winter	5 52	5 71	2 10

2.5. The chi-square test of goodness of fit :

An observed frequency distribution in a sample may often, on general theoretical grounds, be supposed to arise from a true binomial, Poisson, normal, or some other known type of distribution in the population. This hypothesis may be tested by comparing the observed frequencies in various classes with those which would be given by the assumed theoretical distribution. Usually, the parameters of this distribution will not be known from prior considerations but will have to be estimated from the sample It may be shown that if s parameters are estimated by the method of maximum likelihood the limiting distribution of the goodness-of-fit χ^2-statistic defined by

$$\chi_s^2 = \sum_{i=1}^{k} \frac{(O_i - E_i)^2}{E_i} \tag{11}$$

where

O_i = the observed frequencies of the *i-th* class,

E_i = the expected frequencies of the *i-th* class,

$i = 1, 2, ..., k.$

with $k - s - 1$ degrees of freedom (df.).

The estimators used for the parameters need not be the maximum likelihood ones, as long as they are asymptotically normal and most efficient. We have used the estimated frequencies obtained with the method-of-moments estimators of the parameters p and q of the

Table 4. Value of the parameters p and q of beta-distribution and the chi-square value for the year, 1986.

Months	p	q	χ^2
January	5 37	4 75	2 59
February	3 95	4 49	1 55
March	3.15	3.04	6.54
April	2 80	3.59	8 43
May	–	–	–
June	6 12	7.34	10 24
July	7.07	7.43	0 49
August	4.67	4.47	6 03
September	–	–	–
October	4 78	3.34	4 52
November	6.67	10.16	7 96
December	11.36	12 40	1 01

respective beta distributions. The computed χ^2 values for the seasons and months for which unimodal data were obtained are given in Tables 2 and 4 respectively for the year 1986 and in Tables 3 and 5 for the year 1987. Since the tabulated upto 1% and 5% points of the central χ^2 distribution with 5 degrees of freedom are 15.086 and 11.070 respectively, it is apparent from the tables that the fit is *good* in all cases.

Table 5. Value of the parameters p and q of beta-distribution and the chi-square value for the year, 1987

Months	p	q	χ^2
January	5 70	5 03	3 20
February	3.95	4 47	1 99
March	3 12	3 13	5 19
April	3 00	3 83	4 83
May	-	-	-
June	5 71	7 18	10 95
July	6 98	7 32	0 83
August	5 02	4 86	3.12
September	-	-	-
October	6 24	4 30	10 13
November	6 81	10 38	12 25
December	10 86	11.86	3 47

2.6. Fitting of finite mixture distributions to multimodal frequency distributions of VHF signal level :

We have used the Expectation-Maximization (EM) Algorithm, first formalized by Dempster, *et al* [17] in 1977, to fit finite normal mixtures to those frequency distributions of VHF signal level, that were found to be multimodal. A short discussion on this algorithm, as well as its application to the resolution of mixture distributions into components, is made in the following paragraphs. The EM algorithm, which is basically meant for maximum likelihood estimation with incomplete data can be used to solve the problem of resolution of mixtures into components, by first reformulating it as an incomplete data problem.

2.6.1. The EM algorithm for maximum likelihood estimation with incomplete data

Formally suppose that we have a random variable Z whose density function $f(Z \mid \theta)$ depends on a parameter of interest, θ. If Z were observed we could estimate θ by finding that value θ for which $L(\theta \mid Z) \equiv f(z \mid \theta)$ is maximized, with the bonus that the observed information matrix evaluated at this estimate provides information about the precision of θ. Suppose, however, that $Z = (Z_p, Z_m)$, where Z_p is observed (Present) and z_m is not (Missing). An intuitively appealing approach often advocated in the literature is to treat Z_m as if it were an unknown parameter. This "parameter" is estimated (predicted, in other words) and the estimates Z_m are treated as if they had been observed. Thus, θ is then estimated by maximizing $L(\theta \mid Z)$, where $Z \equiv (Z_p, Z_m)$. In effect, we "complete" the data vector and use maximum likelihood with *imputed* the data; this is equivalent to maximizing $f(z_p, z_m \mid \theta)$ with respect to (z_m, θ).

The EM algorithm [17, 18] is most practically useful when the maximum likelihood estimate for θ based on the *complete* data $Z = (Z_p, Z_m)$ is easy to compute. The algorithm is an iterative one, each iteration consisting of two steps. The first part of each iteration is called the *E – step* (for Expectation), in which the expected loglikelihood function of the complete data given the observed data is computed, evaluated at the current estimate for θ, say $\hat{\theta}^{(t)}$. That is, we compute

$$l^{(t)}(\theta) = E\left[\log f(Z_p, Z_m \mid \theta) \mid Z_p, \hat{\theta}^{(t)}\right]. \tag{12}$$

Although in general this involves computing the expected value of a random function, in many practical situations it does not. In particular, if the distribution of Z is from an exponential family, then the right-hand side of equation 5.29 can be reduced to computing the expected value of the complete-data giving sufficient statistic for θ, which is often a one or two dimensional random variable. The second part of each iteration is called the *M-step* (for Maximization), in which the expected log-likelihood just computed is maximized. That is, we compute the updated estimate for θ as that value $\hat{\theta}^{(t+1)}$ which maximizes $l^{(t)}(\theta)$:

$$\hat{\theta}^{(t+1)} \equiv max_\theta^{-1}\ l^{(t)}(\theta) \tag{13}$$

The problem of estimation of the components of finite mixtures can be formulated as an incomplete data problem [17, 18], the missing information being the component to which a given sample belongs. Therefore, in fact, the problem of maximum likelihood estimation of mixture components and mixing proportions is greatly simplified if the problem is so formulated and then solved by means of the EM algorithm

2.6.2. *Finite normal mixtures with univariate component densities*

In the expression for the mixture model given by eq. 1, the g component densities are taken to be univariate normal with unknown means μ_1, ..., μ_g and variances $\sigma_1^2, \sigma_2^2, \ldots, \sigma_g^2$ We henceforth write $f_i(\omega)$ as $f_i(\omega, \theta_i)$, where

$$\theta_i = (\mu_i, \sigma_i^2)^T$$

and

$$\theta = (\mu_1, \ldots, \mu_g, \sigma_1^2, \sigma_2^2, \ldots, \sigma_g^2)$$

contains the distinct unknown parameters in these g normal component densities. The vector Ψ containing all the unknown parameters is now

$$\Psi = (\theta^T, \pi_1, \ldots, \pi_{g-1})^T .$$

The normal mixture model to be fitted is thus

$$f(\omega; \Psi) = \sum_{i=1}^{g} \pi_i f_i\ (\omega; \theta_i),$$

where

$$f_i\ (\omega; \theta_i) = (2\pi\sigma_i^2)^{-1/2}\ exp\ \{-\frac{1}{2}(\omega - \mu_i)^2 / \sigma_i^2\}$$

with

$$\sum_{i}^{g} \pi_i = 1 \tag{14}$$

The estimation of Ψ on the basis of the observation vector y is only meaningful if Ψ is identifiable ; that is, distinct values of Ψ determine distinct members of the family

$$\{f(\omega; \Psi) : \Psi \in \Omega\},$$

where Ω is the specified parameter space. This is true for normal mixtures in that we can determine Ψ up to a permutation of the component labels. For example, for $g = 2$, and $\sigma_1 = \sigma_2 = \sigma^2$ we cannot distinguish $(\pi_1, \mu_1, \mu_2, \sigma^2)^T$ from $(\pi_2, \mu_2, \mu_1, \sigma^2)^T$, but this lack of identifiability is of no concern in practice, as it can be easily overcome by the imposition of the constraint $\pi_1 \le \pi_2$; see McLachlan and Basford [19]. We may refer to Titterington *et al.* [20] for a lucid account of the concept of identifiability for mixtures.

We take the complete-data vector x to be

$$x = (y^T, z^T)^T$$

where the unobservable vector z is defined as follows.

$$Z = (z_1', z_2', \ldots, z_n'),$$

where z_j is a g-dimensional vector of zero-one indicator variables and where $z_{ij} = (z_j)_i$ is one or zero according as whether w_j arose or did not arise from the i^{th} component of the mixture, $i = 1, \ldots, g; j = 1, \ldots, n$.

The complete-data log likelihood function of Ψ is given by

$$\log L_c(\Psi) = \sum_{i=1}^{g} \sum_{j=1}^{n} z_{ij} \log \pi_i + C,$$

where

$$C = \sum_{i=1}^{g} \sum_{j=1}^{n} z_{ij} \log f_i(w_j; \theta_i)$$

$$= -\frac{1}{2} n \log(2\pi)$$

$$-\frac{1}{2} \sum_{i=1}^{g} \sum_{j=1}^{n} z_{ij} \{\log \sigma_i^2 + (w_j - \mu_i)^2 / \sigma_i^2\}.$$

The E-step requires the calculation of

$$z_{ij}^{(k)} = \pi_i^{(k)} f_i(w_j) / f(w_j; \Psi^{(k)}), \quad i = 1, \ldots, g; j = 1, \ldots, n. \tag{15}$$

The M-step now requires the computation of not only

$$\pi_i^{(k+1)} = \sum^{n} z_{ij}^{(k)} / n, \quad i = 1, \ldots, g \tag{16}$$

but also the values $\mu_i^{(k+1)}, \ldots, \mu_g^{(k+1)}$ and $\sigma_1^{(k+1)^2}, \sigma_2^{(k+1)^2}, \ldots \sigma_g^{(k+1)^2}$ that, along with $\pi_1^{(k)}, \ldots, \pi_{g-1}^{(k)}$ maximize $Q(\Psi; \Psi^{(k)})$. Where $Q(\Psi; \Psi^k) = E_\Psi^{(k)} \log L_C(\Psi) / y$. Now

$$\sum_{j=1}^{n} z_{ij} w_j / \sum_{j=1}^{n} z_{ij} \tag{17}$$

and

$$\sum_{i=1}^{g} \sum_{j=1}^{n} z_{ij} (w_j - \mu_i)^2 / \sum_{j=1}^{n} z_{ij} \tag{18}$$

are the MLE's of μ_i and σ_i^2 respectively, if the z_{ij} were observable. As $\log L_c(\Psi)$ is linear in the z_{ij}, it follows that the z_{ij} in eqs. (17) and (18) are replaced by their current conditional expectations $z_{ij}^{(k)}$, which are the current estimates $\tau_i(w_j; \Psi^{(k)})$ of the posterior probabilities of membership of the components of the mixture, given by

$$\tau_i(w_j, \Psi^{(k)}) = \pi_i^{(k)} f_i(w_j; \theta_i^{(k)}) / f(w_j; \Psi^{(k)}) \quad (i = 1, \ldots, g).$$

This yields

$$\mu_i^{(k+1)} = \sum_{j=1}^{n} z_{ij}^{(k)} w_j / \sum_{j=1}^{n} z_{ij}^{(k)} \quad (i = 1, \ldots, g) \tag{19}$$

and

$$\sigma^{(k+1)^2} = \sum_{i=1}^{g} \sum_{j=1}^{n} z_{ij}^{(k)} (w_j - \mu_i^{(k+1)})^2 / \sum_{j=1}^{n} z_{ij} \tag{20}$$

and $\pi_i^{(k+1)}$ is given by eq. (16). It was seen from the data that the VHF level distributions for May and September were bimodal for both the years, namely, 1986 and 1987. So we implemented the above algorithm on the four corresponding data sets with $g = 2$ and the starting value

$$\pi_1^{(0)} = \frac{\overline{X} - \overline{X}_2}{\overline{X}_1 - \overline{X}_2},$$

where the quantities $\overline{X}_1$ and $\overline{X}_2$ are the means of the data subsets lying to the left and right respectively of the X-value corresponding to the valley located in the interior of the distribution The goodness-of-fit test was also done and the fits found to be 'good'. The result are summarised in the following tables.

3. Tropospheric VHF fading rate analysis : monthly and seasonal study

To investigate the fading characteristics, we have estimated the monthly and the seasonal variation of average fading rate of 188 MHz TV signal, travelling over Satkhira-Calcutta link.

Figures 21 to 32 show the variation of the average fading rate with respect to time during the months of January to December respectively. Fading rate provides information on

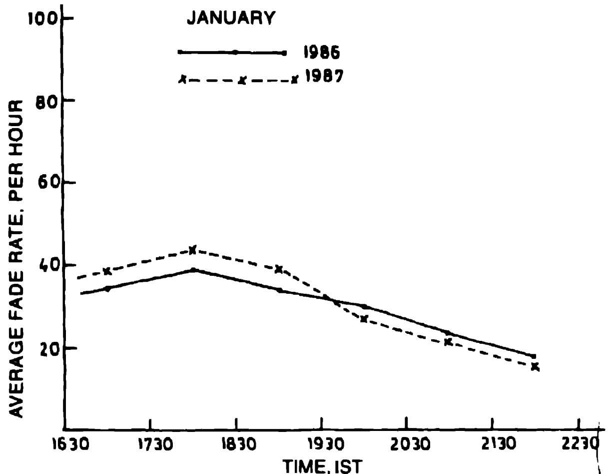

Figure 21. Variation of average fading rate of the 188 MHz VHF signal during the month of January

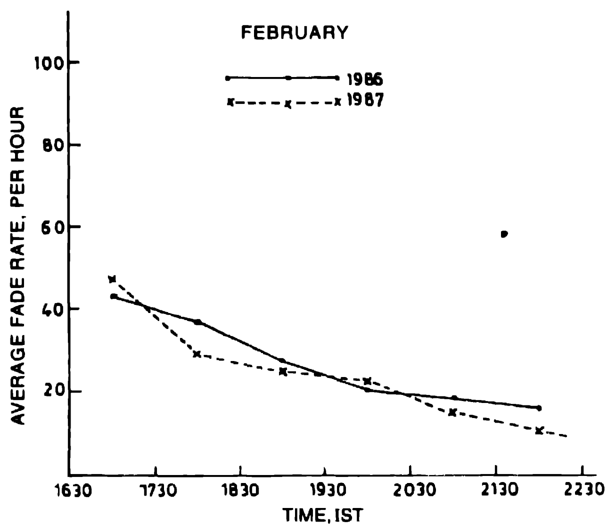

Figure 22 Variation of average fading rate of the 188 MHz VHF signal during the month of February

variation of turbulence factor in tropospheric boundary layer due to corresponding changes in the radiorefractive properties. The fading rate can be defined as the number of times the received envelope of field strength of a signal crosses the mean signal value for a time period of one minute.

We have estimated the number of fades per hour with respect to mean and median VHF signal levels. In the above mentioned figures, the solid curves show the time variation of the average fading rate estimated with respect to the mean VHF signal level, whereas dotted curves show the time variation of the average fading rate estimated with respect to the median VHF signal level. These figures reveal that from the month of January to April the average VHF fading rate has decreased as the transition of time take place from early evening to night hours. This particular characteristics appeared again from the month of September to December. The most significant decrease in the average VHF fading rate has been observed during the night hours of the winter season. Therefore, it has been concluded that fading rate of VHF signal is the least during the night hours of the winter season.

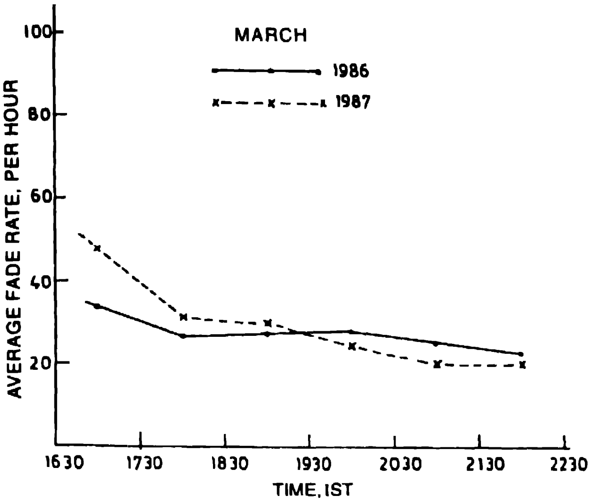

Figure 23 Variation of average fading rate of the 188 MHz VHF signal during the month of March.

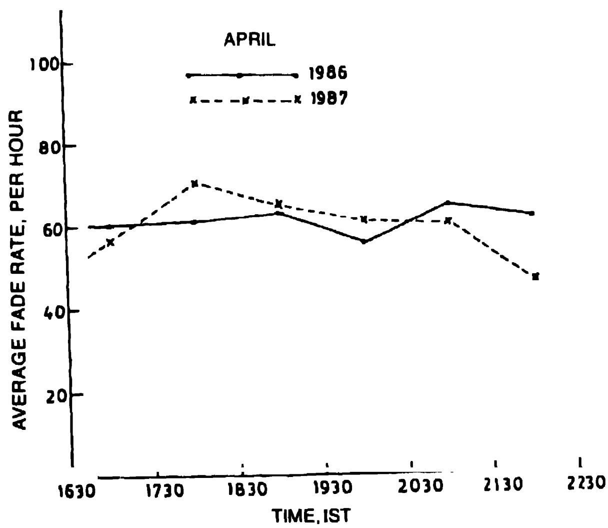

Figure 24. Variation of average fading rate of the 188 MHz VHF signal during the month of April.

On the other hand, during the month of May (peak period of the pre-monsoon season) and the monsoon season (June, July and August) the average VHF fading rate has increased with time. The most significant increase in VHF fading rate has been observed during the month of July when it has reached the value of 95 fades per hour. Therefore, from the above results, it has been concluded that the average fading rate of a 188 MHz VHF signal (propagating between Satkhira-Calcutta, tropospheric LOS link) is maximum during the night hours of the monsoon months.

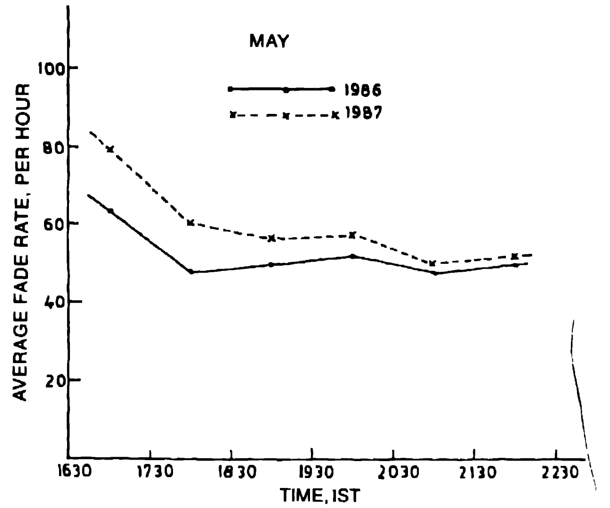

Figure 25 Variation of average fading rate of the 188 MHz VHF signal during the month of May.

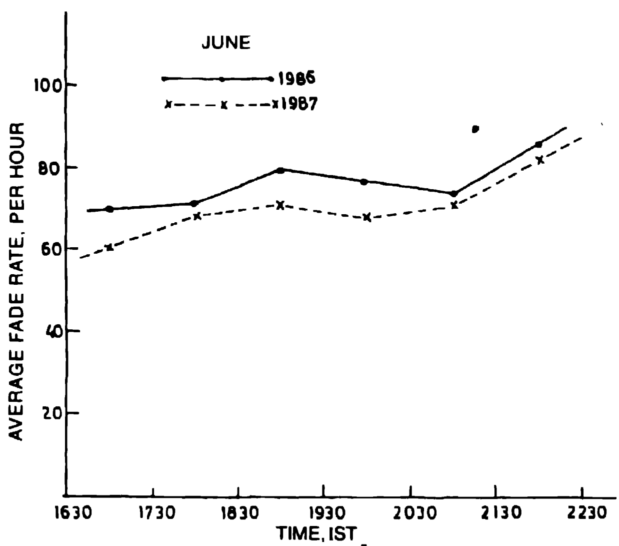

Figure 26. Variation of average fading rate of the 188 MHz VHF signal during the month of June

These discrepancies in the fading behavior of VHF signal can be explained on the basis of the radioclimatic condition of the tropospheric environment over the eastern coastal region of India. In this region, an excessively large number of water vapour molecules remain present in the lower atmosphere during the monsoon season. This high humidity content of the TBL radiates the heat at a slower rate and the process of radiation takes place for a longer duration of time in comparison with the earth surface. At the same time, mutual absorption (heat radiated by a molecule may be absorbed by another molecule and so on) of heat may take place within

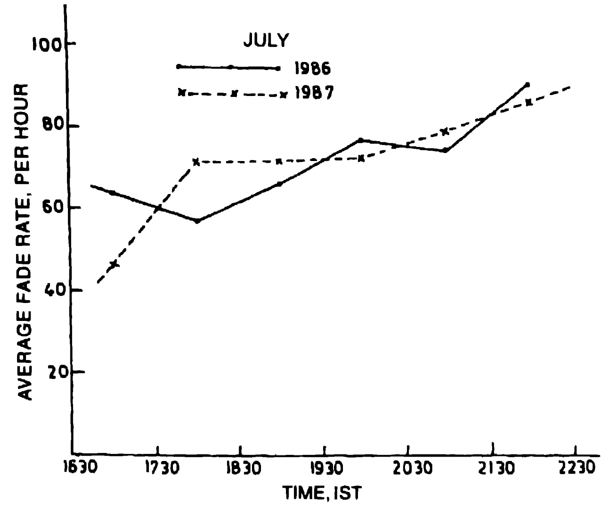

Figure 27 Variation of average fading rate of the 188 MHz VHF signal during the month of July

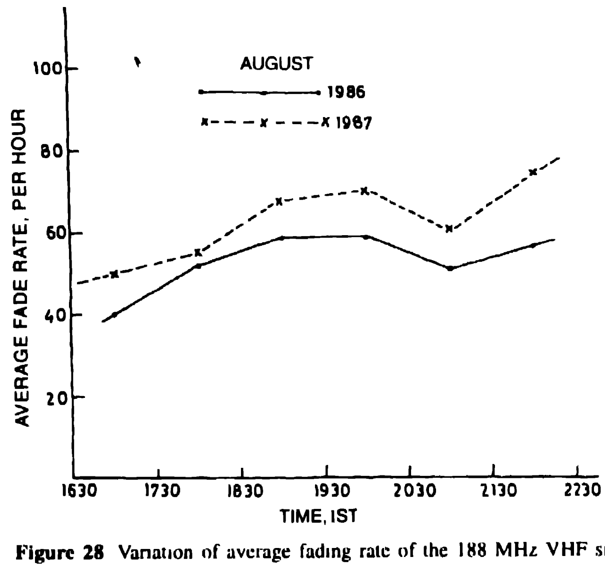

Figure 28 Variation of average fading rate of the 188 MHz VHF signal during the month of August

the different water vapour molecules. This in turn initiates the changes in the thermodynamic state of the lower atmosphere. Changes produced by these large numbers of water vapour molecules may vary at random with time. We already know that any small change in the radio-refractivity (particularly in the wet term) causes a large change in the characteristics of tropospheric radiowave propagation. Thus the changes produced by these huge number of humidity particles introduces a kind of inhomogeneity in the first few hundreds meter of the lower atmosphere. Due to these inhomogeneities, the received signal may not be a single ray but a number of separate and distinct rays each arriving at receiving antenna *via* a slightly different path. Each of these paths is continually changing its shape by small amounts but such changes may correspond to many wavelengths at very high frequencies. The result is

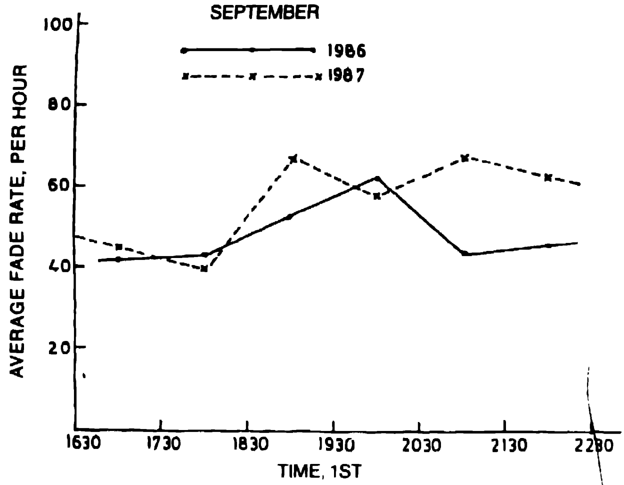

Figure 29 Variation of average fading rate of the 188 MHz VHF signal during the month of September

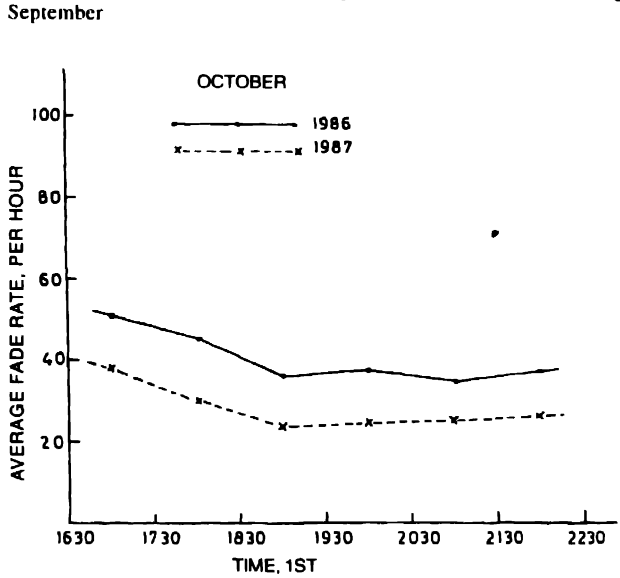

Figure 30 Variation of average fading rate of the 188 MHz VHF signal during the month of October

that, the rays combine with constantly changing phases, thereby leading through constructive interference to large resultant amplitude at some instant and through destructive interference to small ones at others. These fluctuations in resultant amplitudes occur at random and are generally quite rapid. These continuous variation in resultant amplitude can be defined as initiation of fast fading mechanism. Therefore, we may conclude that during the monsoon season existence of large number of humidity particles introduces a kind of inhomogeneity which in turn initiate severe fast fading mechanism of VHF signal, propagating over a tropospheric link situated over eastern coastal region of India.

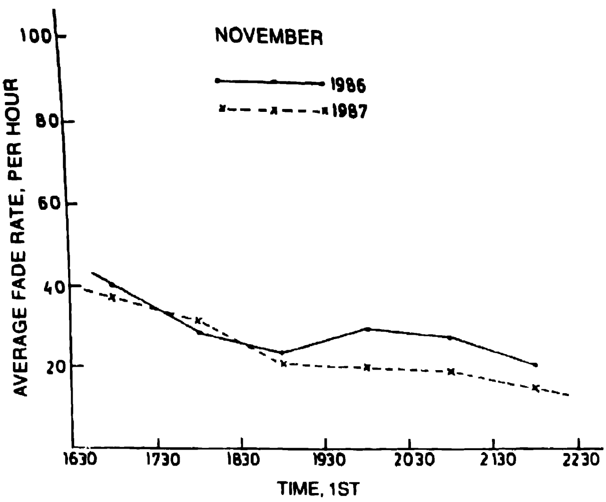

Figure 31 Variation of average fading rate of the 188 MHz VHF signal during the month of November

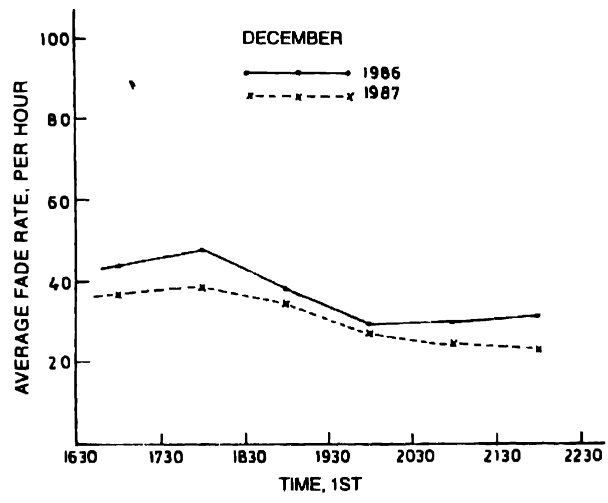

Figure 32 Variation of average fading rate of the 188 MHz VHF signal during the month of December

4. Tropospheric VHF fade depth analysis : monthly and seasonal study

It is a well known fact that the phenomenon of fading take place due to various meteorological causes such as, – changes in the condition of turbulent mixing, fronts, variation in temperature distribution and so on. Key measures to study the fading characteristics are – rate of fading, depth of fading, fade duration *etc.* In the previous section we have discussed about the variation of average fading rate during different months and seasons over the eastern coastal region of India.

Here, we will discuss about the variation of average fade depth with respect to time during different months over the same region. The depth of fading or fade depth can be defined as

$$F_D = E_{0.1} - E_{0.9}, \tag{21}$$

where $E_{0.1}$ is the VHF signal level exceeded during 10 percent of the time and $E_{0.9}$ is the VHF signal level exceeded during 90 percent of the time.

Figures 33 to 44 show the variation of average fade depth with respect to time during the months of January to December respectively. In the above mentioned figures the continuous curves show the variation of average fade depth for the year 1986, whereas the dotted curves describe the variation of average fade depth for the year 1987.

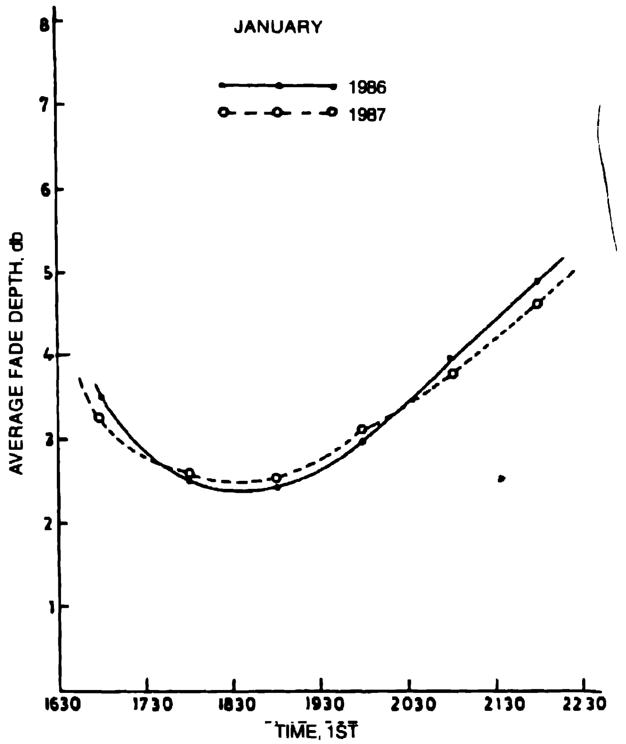

Figure 33. Variation of average fade depth of the 188 MHz VHF signal during the month of January

Figure 33 shows that during the month of January (1986) the minimum and maximum average fade depth are 2.4 db (between 1830 and 1930 IST) and 4.9 db (between 2130 and 2230 IST) respectively. Similarly for January 1987 the corresponding values of the minimum and maximum fade depths are 2.5 db (between 1830 and 1930 IST) and 4.7 db (between 2130 and 2230 IST) respectively. Further investigations reveal that the average fade depth has decreased slowly during early evening hours (between 1630 and 1830 IST) whereas it has increased sharply between 1830 and 2230 IST.

Figure 34 depicts that during the month of February 1986, the values of the minimum and maximum average fade depths are 3.1 db (between 1730 and 1830 IST) and 5.3 db (between 2130 and 2230 IST) respectively. For the year 1987 the corresponding values of minimum and maximum average fade depths are 3.4 db (between 1730 and 1830 IST) and 4.8 db (between 2030 and 2130 IST) respectively. Analogous to the month of January during February the average fade depth has decreased slowly between 1630 and 1730 IST and increased continuously increased from 1730 to 2130 IST.

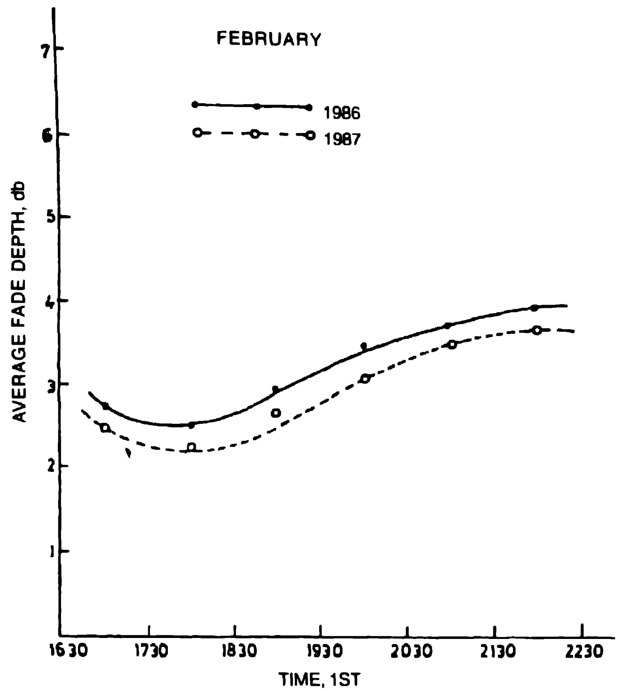

Figure 34. Variation of average fade depth of the 188 MHz VHF signal during the month of February

Figure 35 shows that during the month of March 1986 the minimum and maximum average fade depths are 4.3 db (between 1630 and 1730 IST) and 5.8 db (between 2130 and 2230 IST) respectively. Similarly for the March 1987, the corresponding values of the minimum and maximum average fade depths 3.8 db (between 1630 and 1730 IST) and 5.5 db (between 2130 and 2230 IST) respectively. During the month of March a continuous increase in average fade depth has been observed between 1630 and 2230 IST.

It can be observed from Figure 36 that during the month of April 1986 the minimum and the maximum average fade depths are 6.3 db (between 1730 and 1830 IST) and 8.1 db (between 2130 and 2230 IST) respectively. Similarly in April 1987, the corresponding values are 5.8 db (between 1730 and 1830 IST) and 7.2 db (between 2130 and 2230 IST) respectively. It is noteworthy that during the month of April the minimum average fade depth is greater than the maximum average fade depth observed during the month of March.

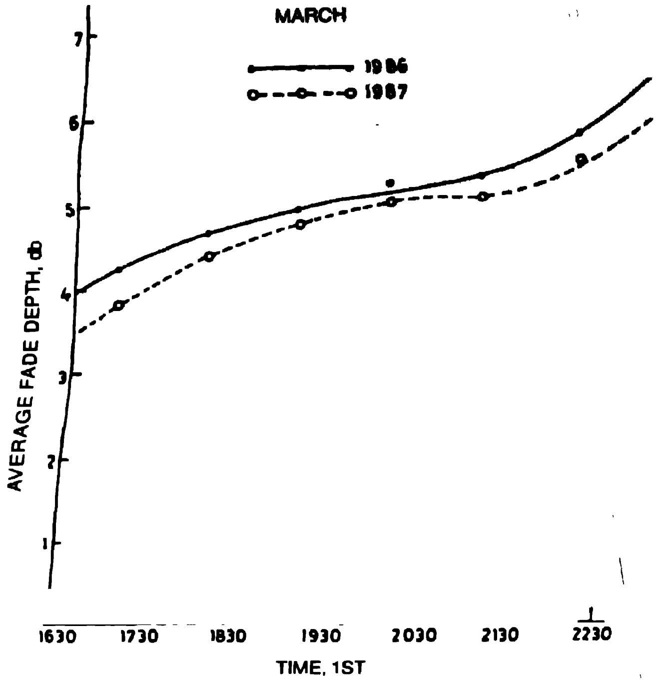

Figure 35. Variation of average fade depth of the 188 MHz VHF signal during the month of March

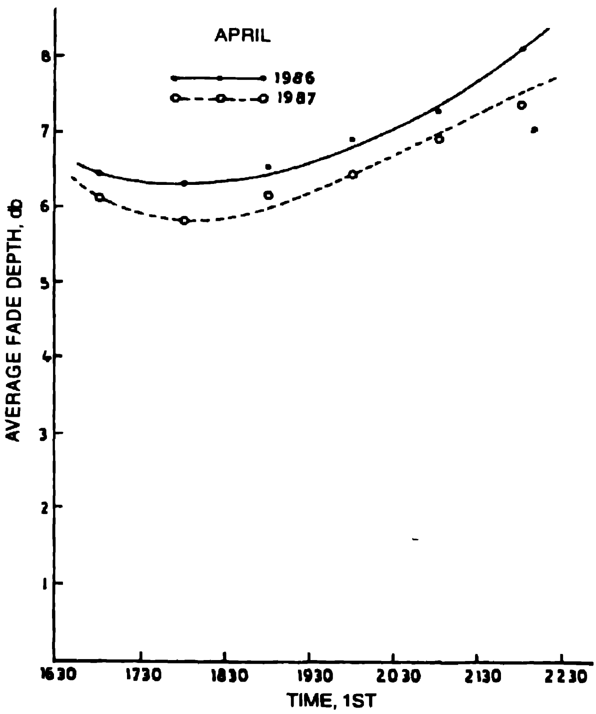

Figure 36. Variation of average fade depth of the 188 MHz VHF signal during the month of April

Figure 37 shows that during the month of May 1986, the average fade depth has fluctuated between 6.1 db and 7.2 db and for the year 1987 the corresponding range of variation is 5.8 db to 7.3 db. For the month of May, likewise the month of April, the average fade depth has attained a higher value (of the order of 6 to 7 db) during the entire course of observation.

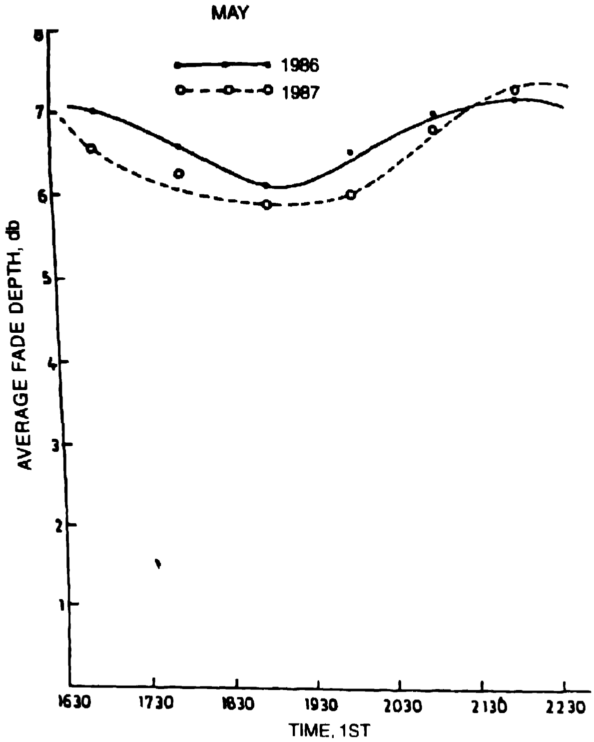

Figure 37. Variation of average fade depth of the 188 MHz VHF signal during the month of May.

Figure 38 suggests that during the month of June 1986 the average fade depth is the maximum (4.1 db) between 1730 and 1830 IST and the minimum (3.1 db) between 2130 and 2230 IST. Similarly, for the year 1987, the corresponding values of the maximum and the minimum average fade depths are 4.4 db (1730–1830 IST) and 2.8 db (2130–2230 IST) respectively. From the above discussion it follows that during the month of June, the range of variation of average fade depth is much smaller than that observed during pre-monsoon months (March, April and May).

Figure 39 shows that during the month of July 1986 the average fade depth is the maximum (2.2 db) between 1730 and 1830 IST and the minimum (1.9) db between 1930 and 2030 IST. Similarly for the year 1987 the corresponding values of the maximum and minimum average fade depths are 2.2 db (1930-2030 IST) and 1.7 db (1630-1730 IST) respectively. Further investigation reveals that in July the range of variation of the average fade depth has been narrowed further.

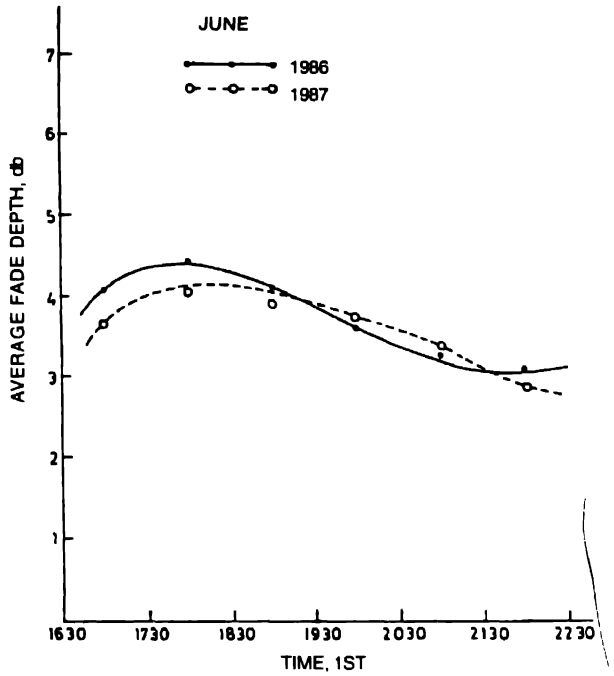

Figure 38. Variation of average fade depth of the 188 MHz VHF signal during the month of June

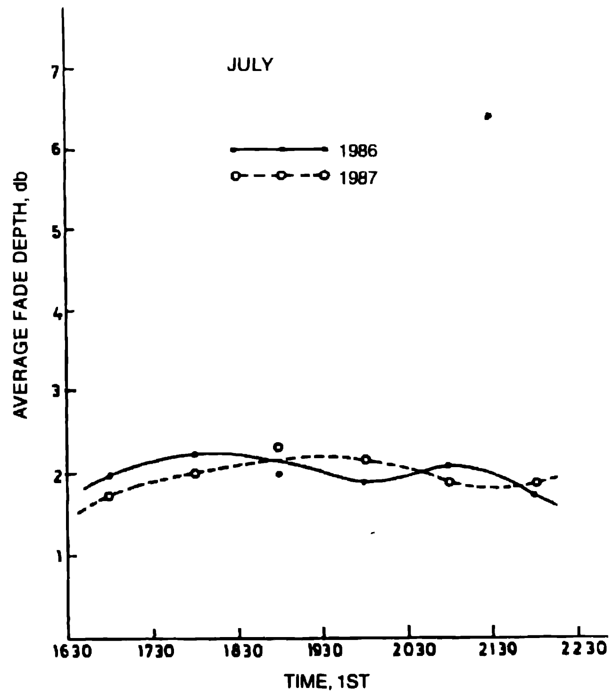

Figure 39. Variation of average fade depth of the 188 MHz VHF signal during the month of July

Figure 40 depicts that in August 1986, the values of the maximum and the minimum average fade depths are 2.5 db (1630–1730 IST) and 1.4 db (2130–2230 IST) respectively. Similarly, for the year 1987 the corresponding maximum and minimum values of average fade depths are 2.3 db (1630–1730 IST) and 1.3 db (1830–1930 IST) respectively. As in the month of July, during the month of August also the average fade depth has attained a lower value (of the order of 1.5 db to 2.5 db) during the entire course of observation.

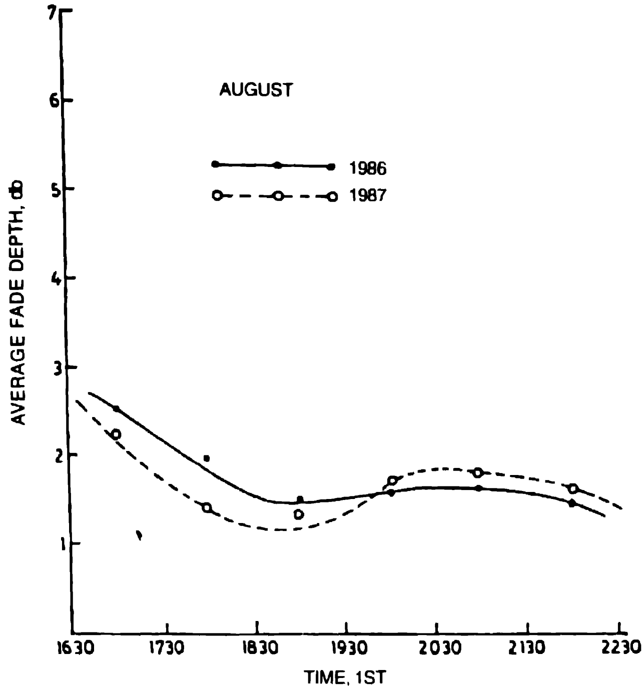

Figure 40. Variation of average fade depth of the 188 MHz VHF signal during the month of August

Figure 41 describes that during the month of September 1986, the average fade depth has decreased during the early evening hours (1630–1730 IST) whereas during later hours it has experienced small variations with respect to time. During this month, the values of the maximum and the minimum average fade depths are 4.0 db (1630–1730 IST) and 3.0 db (2130–2230 IST) respectively. Similarly, in September 1987, the corresponding values are 3.9 db (1630–1730 IST) and (1730–1830 IST) respectively.

Figure 42 suggests that similar as in the month of January, during the month of October the average fade depth has decreased between 1630 to 1830 IST whereas it has increased continuously between 1830 to 2230 IST. During October 1986, the maximum and minimum average fade depths are 4.7 db (2130–2230 IST) and 3.2 db (1730–1830 IST) respectively. Similarly, for the year 1987, the corresponding values are 4.0 db (2130–2230 IST) and 2.7 db (1730–1830 IST) respectively.

Figure 43 shows that in November, the average fade depths has increased slowly during evening hours (1630–1730 IST) and has decreased gradually between 1930 to 2230 IST. In

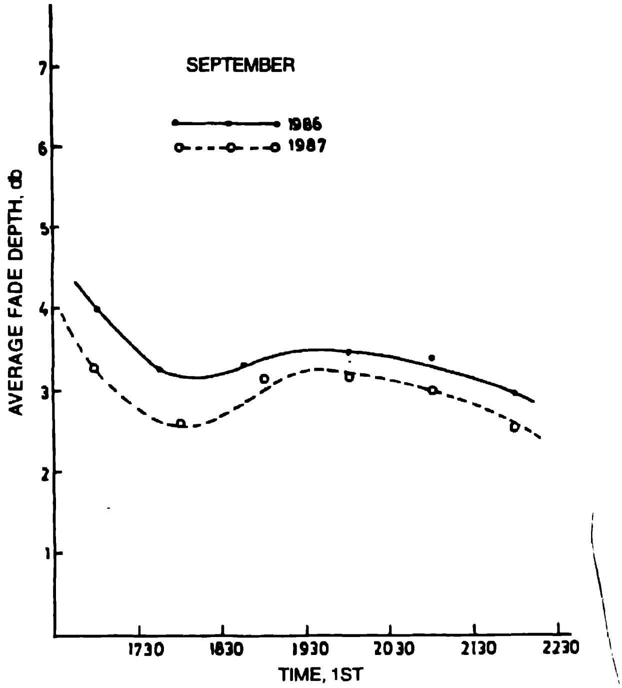

Figure 41. Variation of average fade depth of the 188 MHz VHF signal during the month of September

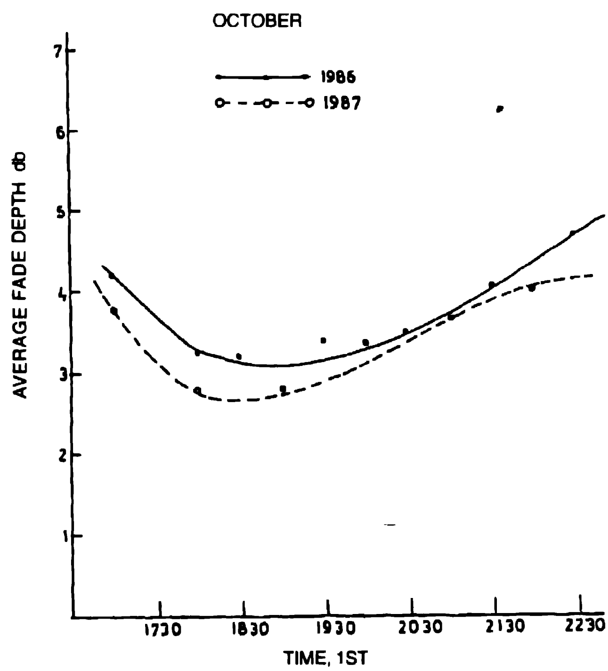

Figure 42. Variation of average fade depth of the 188 MHz VHF signal during the month of October.

November 1986, the values of the maximum and the minimum average fade depths are 3.8 db (1830–1930 IST) and 2.7 db (2130–2230 IST) respectively. Similarly, for the year 1987, the corresponding values are 3.2 db (1730–1830 IST) and 2.3 db (2130–2230 IST) respectively.

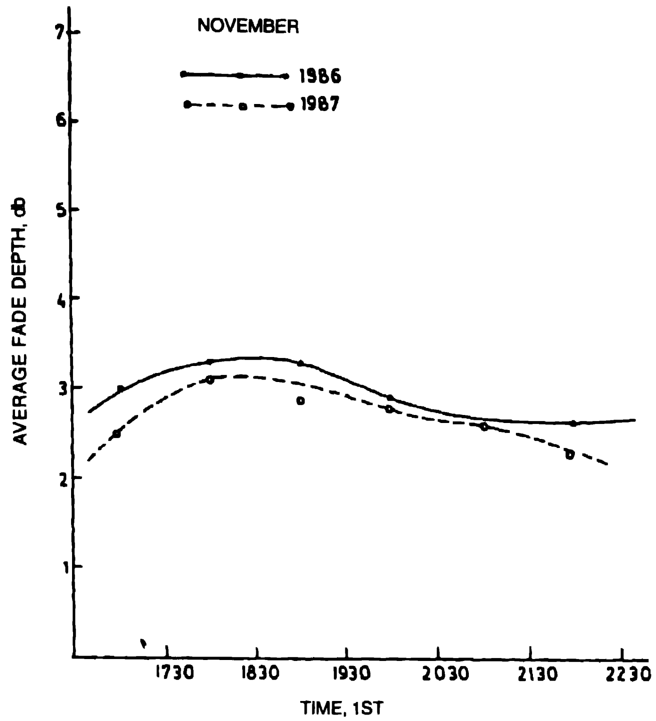

Figure 43. Variation of average fade depth of the 188 MHz VHF signal during the month of November

It can be seen from Figure 44 that during the month of December the average fade depth has decreased initially between 1630 to 1930 IST and has increased sharply between 1930 to 2230 IST. During November 1986 the values of the maximum and the minimum average fade depths are 4 db (2130–2230 IST) and 2.9 db (1730–1830 IST) respectively. Similarly, during December 1987, the corresponding values are 4.3 db (2130–2230 IST) and 2.6 db (1830–1930 IST) respectively.

The above experimental results show that the pre-monsoon season exhibits the highest value of the average fade depth and the monsoon season depicts the lowest value, whereas fade depth values for the winter season are higher than those of the post monsoon season. All these seasonal discrepanices in fading characteristics of VHF signal can be explained on the basis of radioclimatic condition of the corresponding radioenvironment through which the signal is propagating.

From the analysis of radiosonde and sodar observations we have already observed that the probability of formation of superrefractive and ducting gradients are high during pre-monsoon and winter seasons, whereas it is least during the monsoon season [11]. During the winter season, these highly superrefractive gradients are formed mainly due to radiative cooling of the earth surface. In winter nights, once these superrefractive and ducting gradients are formed, this persist for a longer duration of time. On the other hand, during the pre-monsoon season, apart from inversion due to radiative cooling, there exist some other effects which may participate at a higher rate to produce highly superrefractive gradients in the lower tropospheric

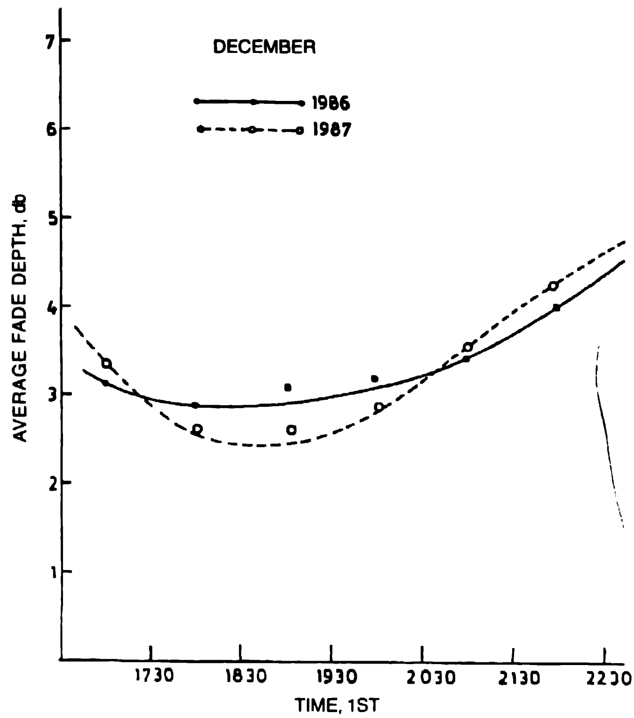

Figure 44. Variation of average fade depth of the 188 MHz VHF signal during the month of December

region. Thus, for instance, during pre-monsoon season, sea breeze effect is dominant over the coastal region and its surroundings due to the intensive solar heating of the earth surface during the day time. At the same time, drainage of the north easterly flow from the Brahmaputra valley and the north-westernly flow from Chotanagpur plateau, in combination with moisturised air and intensive solar heating of the soil, produces severe thunderstormic activities during the evening hours of the pre-monsoon season over the eastern coastal region of India. It has been observed that departure of these seasonal thunderstorms is generally associated with the formation of superrefractive gradients in the lower atmosphere. Therefore, it is expected that during pre-monsoon and winter seasons due to formation of superrefractive and ducting gradients (on the ground and in the elevated level) the radiowave may not be a single ray (direct ray travelling between a pair of antenna) but a number of separate and distinct rays, involving reflection due to existence of these layers. As a result these rays (direct ray and reflected rays) may combine with constantly changing phases which in turn, introduces rapid fluctuation in the amplitude of resultant wave and occurrence of phenomenon of multipath fading can be observed at the receiver site. Due to occurrence of multipath fading the average fade depth of a VHF signal increases accordingly.

5. Conclusion

A study on propagation characteristics of 188 MHz VHF signal, during different seasons and months over the eastern coastal region of India, has led to the following conclusions :

1. Computation of percentage occurrence of average VHF signal during different seasons over the eastern coastal region reveals that the pre-monsoon season exhibits the highest signal values, followed by the winter season. This is followed by the post-monsoon season, with the monsoon season exhibiting the lowest value.

2. Excepting the months of May and September, during rest of the months, and for the four different seasons the average value of VHF signal level follow a two parameter beta-distribution. On the other hand during the months of May and September it follow a mixture of normal distribution.

3. The fading rate of the VHF signal decreases from January to April and again from September to December. The most significant decrease in average fade rate of the VHF signal has been observed during the night hours of the winter season.

4. The average fading rate of the VHF signal has increased during the months of May, June, July and August The most significant increase in the average fading rate of VHF signal has been observed during the night hours of the month of July.

5. The monthly study reveals that the average fade depth of the VHF signal is maximum and minimum during the months of April and January respectively. On the other hand, the seasonal study describes that pre-monsoon and monsoon season exhibit the highest and lowest values of average fade depths respectively, whereas during the winter season, values of average fade depth of VHF signal are higher than those observed in the post-monsoon season.

References

[1] Livingstone, *Physics of the Microwave Propagation* (Englewood, New Jersy Prentice Hall) (1970)

[2] L Boithias *Radiowave Propagation* (North Oxford Academic) (1987)

[3] J A Schiavone *Radio Sci* **17** p 1301 (1982)

[4] J A Schiavone *Radio Sci.* **18** p 369 (1983)

[5] A P Mitra, B M Reddy and S Agarwal *Tropospheric Propagation and Antenna Measurements* (New Delhi-12, India National Physical Laboratory) (1972)

[6] S C Majumder *Radio and Electronic Engg.* **44** p 63, (1974)

[7] S K Sarkar *Radioclimatological Effects on Tropospheric Radiowave Propagation over Indian Subcontinent* (PhD thesis, Delhi University, India) (1978)

[8] D N Rao *Radioclimatology and Microwave Propagation over Southern India* (PhD thesis, S V University, India) (1984)

[9] M Prasad *Some Aspects of VHF and Microwave Propagation Over Selected Regions of India and Their Application to Communication*, CENTROP Rep 50 (National Physical Laboratory, New Delhi, India) (1989)

[10] *Statistical Studies on Tropospheric Propagation for UHF/VHF and Microwave Links Tech. Rep* (Indian Statistical Institute, Calcutta, India) (1987)

[11] S Choudhury *Tropospheric VHF Propagation Studies Using Ground-Based in-situ and Acoustic Remote Sensing Techniques* (PhD thesis, Submitted to the University of Calcutta) (1998)

[12] S Choudhury, A Pal and D D Majumder *IEE Proc. on Microwave, Antenna and Propagation* (communicated) (1998)

[13] J Das, A K De, N C Deb, D D Majumder, A K Sen, S K Sarkar, H N Dutta and B M Reddy *Indian J Radio Space Phys.* **18** p10 (1989)

[14] J Das, A K De, D D Majumder, A K Sen and S K B Mallick *Indian J Phys.* **63B** 149 (1989)

[15] J Das, A K De and D D Majumder *Int J Remote Sensing* **10** W7 (1989)

[16] N Johnson and S Kotz *Distributions in Statistics* (New York : John Wiley) (1972)

[17] A P Dempster, N M Laird and D B Rubin *J. Royal Stat. Soc.* **B 39** p1 (1977)

[18] G J McLachlan and T Krishnan *The EM Algorithm and its Extensions* (New York : Wiley) (1997)

[19] G J McLachlan and K E Basford *Mixture Models : Inference and Applications to Clustering* (New York Marcel Dekker) (1988)

[20] D M Titterington, A F M Smith and U E Makov *Statistical Analysis of Finite Mixture Distributions* (New York : Wiley) (1985)

ABOUT THE REVIEWERS

Dwijesh K. Dutta Majumder

Dwijesh K. Dutta Majumder obtained his M.Sc(Tech) degree in Radio Physics and Electronics and Ph.D in Digital Computers' Memory Technology in 1955 and 1962 respectively from Calcutta University. Since 1955 he has been working in ISI in different capacities and was Professor and Head of Electronics and Communication Sciences Unit for 20 years. In 1992 Prof. Dutta Majumder was made Professor Emeritus of ISI, Emeritus Scientist of CSIR and Chairman of the National Center for Knowledge Based Computing at ISI. He is Secretary-Director of the newly started Institute of Cybernetics, System and Information Technology (ICS ANDIT) at Salt Lake Electronic complex, Calcutta. He is the author of more than 450 research papers in international journals and conference proceedings and is the author/editor of six books all published by John Willey and Sons in the area of memory technology, pattern recognition, man-machine communication expert system, image processing, computer vision, data communication, atmospheric sciences, neural modeling and fuzzy mathematics.

Professor Dutta Majumder visited and delivered lectures on his work in some of the above mentioned subjects in large number of universities and industrial labs in USA, U.K., Japan and Europe as a Guest Professor several times. He is a member of the editorial boards of Pattern Recognition Letters (PRL), The International Journal of Fuzzy Mathematics (USA), Indian Journal of Pure and Applied Mathematics (IJPAM), International J. of Image Processing and Communication (Poland) and was the consulting editor of the Journal of Computer Division of the Institution of Engineers (India).

Prof. Dutta Majumder is a Fellow of International Association of Pattern Recognition (IAPR), Indian National Science Academy, Indian National Academy of Engineering, The National Academy of Science, Computer Society of India and Institution of Electronics and Telecommunication Engineering and is a member of the Governing Board of IAPR and International Fuzzy Systems Association (IFSA), Director of World organization of Cybernetics and System (WOSC), President of Indian Society of Fuzzy Mathematics and Information Processing (ISFUMIP) and Indian Unit for Pattern Recognition and Artificial Intelligence (IUPARI). He is recipient of Sir J. C. Bose Award of IETE, Sir C. V. Raman award of ASI, Norbert Wiener Award of WOSE, R. L. Wadhwa Gold Medal of IETE, P. C. Mahalanobis Gold Medal of INSA, Jawaharlal Nehru Birth Centenary Award of INSA, K. S. Krishnan Gold Medal of IETE and several other honours and awards.

Swati Choudhury

Swati Choudhury received her M.Sc degree in Physics (Electronics) from Rohilkhand University, Bareilly (U.P). She attended M. Phil course in Physical Science at S N. Bose Institute of Physical Sciences (Calcutta). For her research, she joined Electronics and Communication Sciences Unit of Indian Statistical Institute (Calcutta) and submitted her Ph.D. Thesis in the area of Radio Physics and Electronics. She has worked as JRF/SRF and Research Assistant in different *R&D* projects funded by DST, New Delhi and ISI, Calcutta. Presently she is working as Visiting Scientist in Machine Intelligence Unit of ISI, Calcutta. Her area of research interest includes radio-communication, atmospheric remote sensing, radio-climatology, environmental pollution studies and boundary layer studies using standard statistical and mathematical modeling methods.

Amita Pal

Working as a lecturer in the Applied Statistics Unit of the Indian Statistical Institute since 1994, having obtained her M. Sc. degree from the University of Calcutta in 1981 and her Ph. D. degree from the Indian Statistical Institute in 1991. Visited the Department of Mathematics of the Imperial College of Science, Technology and Medicine, London, as a UNDP fellow in 1994. Her interests are mainly in the areas of pattern recognition, machine learning and Bayesian image processing.